Limited-angle X-ray tomography for weld inspection

Esa Niemi[a,b], Aaro Salosensaari[a,c], Alexander Meaney[a], Henrik Lohman[d], Samuli Siltanen[a,*]

[a]*Department of Mathematics and Statistics, P.O. Box 68, FI-00014 University of Helsinki, Finland*
[b]*Eniram Ltd., Hiililaiturinkuja 2, FI-00180, Helsinki, Finland*
[c]*Department of Clinical Medicine, Faculty of Medicine, FI-20014 University of Turku, Finland*
[d]*Direct Conversion / Oy Ajat Ltd, Tekniikantie 4b, FI-02150, Espoo, Finland*

Abstract

X-ray imaging of long, pipe-like structures often lead to limited-angle tomography problems because of geometric restrictions and high attenuation of the pipe material (for example steel). Tomographic reconstructions from such data are typically inaccurate in the direction perpendicular to the cylindrical axis. For example, small but significant voids in weldings may go unnoticed due to their erroneous elongation in the reconstruction. This inaccuracy may be compensated by prior information on the target being imaged. The reconstruction scheme proposed in this work makes use of the following prior information: (1) the target consists of a small number of known materials, (2) the structure of the target is homogeneous within each material, and (3) the shape of the target is roughly known. Numerical results presented for simulated and real X-ray data demonstrate a significant increase in depth resolution compared to standard tomosynthesis reconstructions.

Keywords: limited-data X-ray tomography, pipes, welding defects, depth resolution, discrete tomography

*Corresponding author

Email addresses: esa.niemi@eniram.fi (Esa Niemi), aaro.salosensaari@iki.fi (Aaro Salosensaari), alexander.meaney@helsinki.fi (Alexander Meaney), henrik.lohman@directconversion.com (Henrik Lohman), samuli.siltanen@helsinki.fi (Samuli Siltanen)

1. Introduction

Non-destructive testing (NDT) is crucial for ensuring the integrity of pipework and welded joints in safety-critical applications such as nuclear power plants. One of the frequently used NDT techniques is X-ray imaging. Due to geometric limitations as well as restrictions in imaging time, X-ray NDT of pipelines often leads to a limited-angle X-ray tomography problem, which is a severely ill-posed inverse problem. Ill-posedness means extreme sensitivity to modelling errors and measurement noise, and *regularized* reconstruction methods are needed for robust and reliable imaging.

Limitations in measurement geometry may also come from the X-ray sensor technology. One of the motivations of this work is the use of CdTe-based direct conversion X-ray detectors in NDT. These detectors typically are tall but narrow in shape, which needs to be taken into account in the design of the measurement setup. A natural way of using these detectors in pipe examinations is to use them in a tomosynthesis type setup such as that used in [1], leading to a limited-angle X-ray tomography problem. See Figure 1 for an illustration.

Limited-angle X-ray tomography problems are known to be severely ill-posed [2, 3, 4, 5, 6]. Regularized reconstruction algorithms for them have been considered extensively in the fields of computational and medical imaging during the last few decades [7, 8, 9, 10, 11, 12, 13, 14, 15]. There are also many recent works studying their application specifically to NDT [16, 17, 18, 19, 20]. The ill-posedness of the limited-angle problems are due to the lack of information in the measurement data. This deficiency can be fixed by using a priori information about the target [6].

In this work we aim to improve the results obtained in [1] for the NDT of welded pipe joints by replacing the standard tomosynthesis reconstruction algorithm by a reconstruction scheme that employs three different types of a priori information about the pipe and/or weld being studied:

(C1) The target consists of a few (say, two or three) different materials.
(C2) The materials are homogeneous and the interfaces between them are sharp.
(C3) The (exterior) shape of the target is known with moderate accuracy.

We enforce (C1) and (C2) by using a slightly modified version of the TVR-DART algorithm introduced in [21] for reconstruction. The main novelty is imposing the condition (C3), which makes a crucial difference in the welding

inspection application. We model the wall of the pipe closer to the X-ray source as uniform material (metal), and choose as degrees of freedom in the optimization problem only pixels in the pipe wall closer to the X-ray detector as free variables.

A similar type of idea of using structural prior information was applied in [22]; however, there the structural prior information was obtained with an additional surface scan, whereas we assume here that the pipe and its dimensions are known rather accurately without additional scans. This assumption is valid in many cases where pipelines or welded pipe joints are being evaluated.

We present numerical results for the proposed computational algorithm using a simulated and a real data test case. The results are compared to standard tomosynthesis reconstructions.

2. Methods and materials

2.1. X-ray measurement setup

In addition to the geometric limitations imposed by the structure of a long pipe, we also assume that the X-ray detector used in the measurements is tall but narrow in shape. This kind of shape is typical to direct conversion X-ray detectors based on CdTe technology. For example, 10 cm $\times$ 1 cm is a typical detector size.

A natural way to use this type of detectors in pipework NDT is a tomosynthesis type measurement setup analogous to the one used e.g. in [1], see Figure 1.

In this article we consider the reconstruction problem only in 2D, but the proposed setup can easily be extended to 3D by rotating the X-ray source and detector around the pipe for each source position. In fact, the resulting 3D reconstruction problem is even easier (more stable) to be solved computationally, since the third dimension brings in more information about the defects.

We shall employ the above kind of measurement setup both in our simulated and real data test cases.

2.2. Reconstruction algorithm

We model the X-ray tomography problem with the matrix equation

$$Ax = m, \tag{1}$$

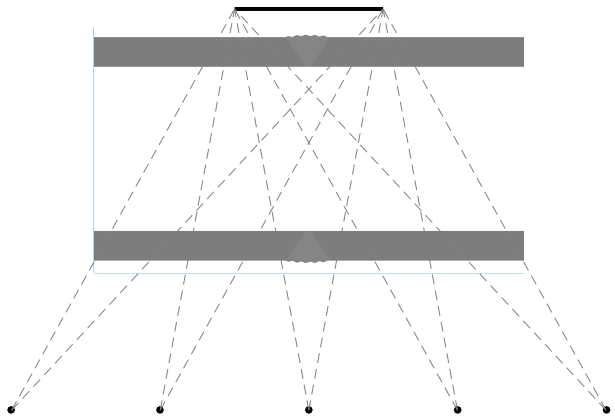

Figure 1: A tomosyntesis type measurement setup using a 10 cm $\times$ 1 cm X-ray detector for the NDT of a 20 mm thick pipe with 150 mm diameter. The pipe has a welded joint in the region of interest close to the detector. The detector is plotted as a thick black line and the source positions are denoted by the black dots. The number of X-ray projections is five, and the total movement of the source is 400 mm.

where $A \in \mathbb{R}^{M\times N}$ is a matrix modeling the measurement process, $x \in \mathbb{R}^N$ denotes the unknown pipe object to be reconstructed and $m \in \mathbb{R}^M$ is the X-ray data. As an important remark we note, that here x contains only the pixels that are known (recall (C3) from Introduction) to belong to the pipe wall that is closer to the detector and that m is the measured X-ray data subtrated by the X-ray attenuation data caused by the pipe wall closer to the X-ray source. Note also that if the object being imaged is a welded pipe joint, then the a priori knowledge of the shape of the weld area might not be very accurate; however, our numerical tests suggest that minor inaccuracies related to the shape of the target do not affect the numerical results too much.

As mentioned in Introduction, we assume that the target consists of a few different homogeneous materials (C1) and the materials are uniform (C2). These pieces of information are taken into account by employing a slightly modified version of the TVR-DART reconstruction algorithm [21]. The modified algorithm finds the reconstruction $x \in \mathbb{R}^N$ as (a) minimizer

$$\arg\min_{x\in\mathbb{R}^N}\{\|AS(x) - m\|_2^2 + \alpha \mathrm{TV}_\beta(x)\},$$

where $S : \mathbb{R}^N \to \mathbb{R}^N$ is a soft segmentation function given by

$$S(x) = \sum_{g=2}^{G} (\rho_g - \rho_{g-1}) u(x - \tau_g, k_g),$$

with

$$u(x, k_g) = \frac{1}{1 + e^{-2k_g x}}, \quad k_g = \frac{K}{\rho_g - \rho_{g-1}}.$$

Here $\alpha > 0$ is a regularization parameter, G is the number of materials and K is called a transition constant; our numerical tests indicate that K values ranging approximately from 3 to 6 seem to work well in computations. In this work we only consider the case $G = 2$, i.e. materials present in the unknown are gas and metal. The parameters ρ_g are the pre-known attenuation values of the materials in the unknown object (e.g. metal and gas) and τ_g are the threshold levels between the different attenuations with $\tau_1 = 0$. Above TV_β denotes a smooth approximation for 2D total variation penalty given by

$$\mathrm{TV}_\beta = \sum_i \sqrt{(x_{i+1} - x_i)^2 + (x_{i+n} - x_i)^2 + \beta}, \quad \beta > 0,$$

where n is the number of rows in the image. We use $\beta = 1e-4$ in numerical computations and find the minimizer with Barzilai-Borwein method [23]. Similarly to [21], standard TV reconstruction is used as the starting point of the iterative minimization. On the edges of the pipe wall we apply zero boundary condition.

There are four differences between this algorithm and the original TVR-DART introduced in [21]. In [21] the (smoothened) TV penalty was applied to $S(x)$ as we apply it to x. We chose the latter option since our computational tests suggested that it leads to more stable numerical results. An additional difference is that in [21] the TV penalty was smoothened using a Huber approximation while we use here the β-smoothing as described above. We expect this does not make essential difference in the results. Thirdly, the minimization method used in [21] was different than ours but essentially both of them are gradient-based methods. Finally, in [21] the attenuation values ρ_g and thresholds τ_g were automatically estimated from the data while we assume they are known a priori.

2.3. Simulated X-ray data

In order to test the proposed reconstruction algorithm we simulate X-ray data for a welded pipe joint phantom with a void of 3 mm diameter, see the top image in Figure 2. The diameter and wall thickness of the pipe are 150 mm and 20 mm, respectively. The measurement setup is the same as that shown in Figure 1. In particular, the total source movement is 400 mm with 80 mm translational step, i.e. the number of projection images is five. The distance between the pipe and the detector is 20 mm and the distance from the source to the axis of the pipe is 175 mm. To simulate measurement errors, we add 2% additive Gaussian noise to the data.

2.4. Real X-ray data for an alumimium pipe

For a real-data test case, we measured X-ray data for an aluminium pipe with 200 mm length, 50 mm outer diameter and 2 mm wall thickness. To create a void inside the pipe, we first cut the pipe into two 100 mm long pieces, made the cutting surfaces perfectly flat by machining and drilled a hole with 0.5 mm diameter to the other flat surface. Finally, the two 100 mm pieces were put together with an aluminium tape so that the flat surfaces were against each other and the 0.5 mm hole was located inside the pipe.

The X-ray data was measured with a custom-built μCT device nanotom supplied by Phoenix—Xray Systems + Services GmbH (Wunstorf, Germany), making use of a CMOS flat panel detector with 2304 $\times$ 2284 pixels of 50 μm size (Hamamatsu Photonics, Japan). For each X-ray image, the detector was translated in horizontal direction 12 cm to both right and left, leading essentially to 36 cm $\times$ 12 cm detector area. The pipe was positioned in front of the detector to five different locations with roughly 3 cm translational step. For each of the locations a 36 cm $\times$ 12 cm projection image was composed as an average of ten 1000 ms exposures. The X-ray tube was stationary during all the measurements and its acceleration voltage was 70 kV and tube current 150 μA. Since we consider here the reconstruction problem in 2D, we only make use of each projection image's middle row corresponding to the central 2D cross-section of the pipe.

3. Computational results

In this section we present numerical results obtained by applying the proposed reconstruction algorithm to the simulated and real X-ray data sets described in the previous section. The results are compared to standard

tomosynthesis reconstructions. X-ray projections and backprojections were computed using Astra Tomography Toolbox [24, 25].

Reconstructions for the simulated data of a welded pipe joint with 3 mm void are shown in Figures 2 and 3. Results for the real X-ray data of an aluminium pipe with 0.5 mm void can be found in Figure 4.

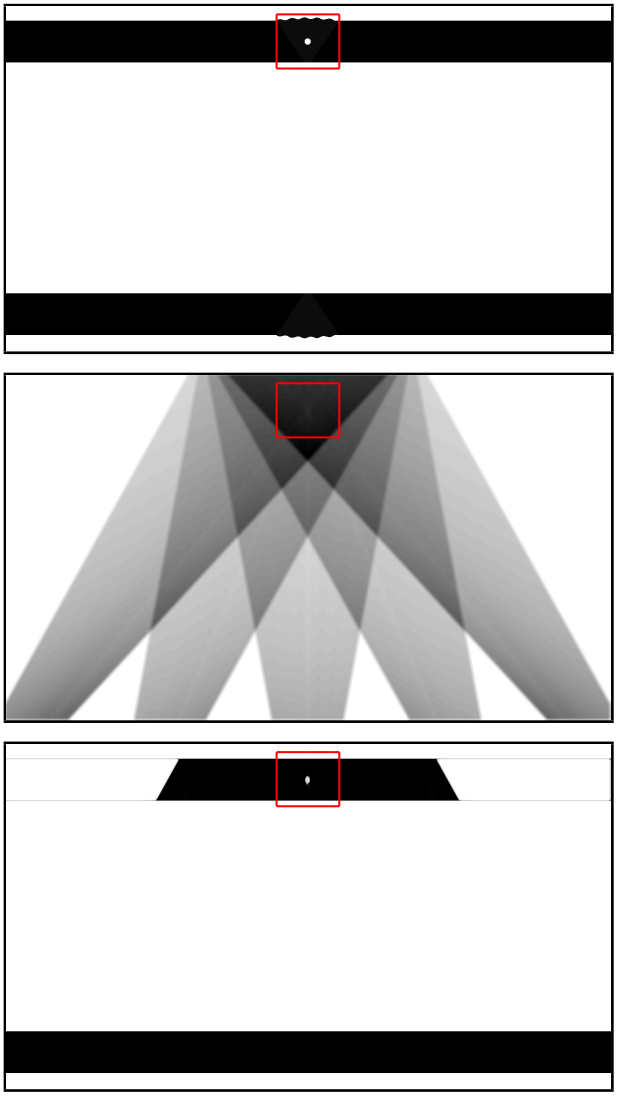

Figure 2: Original phantom (top), tomosynthesis (middle) and the proposed TVR-DART reconstruction (bottom) for simulated data. The areas enclosed by red rectangles are shown in detail in Figure 3. Note that the reconstruction by the proposed method does not precisely follow the shape of the weld; this is due to the fact we assume no accurate a priori knowledge the shape of the weld but use a simple straight-wall approximation.

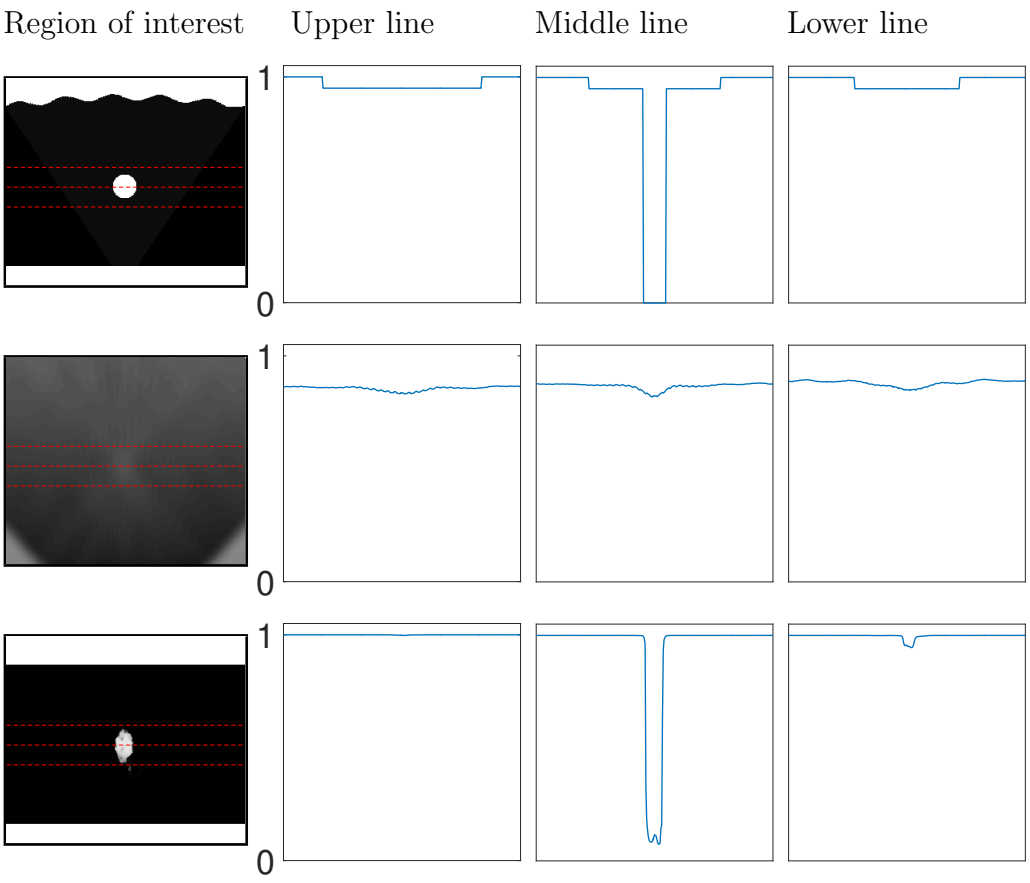

Figure 3: Left column: The regions of interest (ROI) indicated by the red rectangles in Figure 2. On the right of each ROI, profiles corresponding to the red dashed lines in the ROIs. The lines lie 1 mm above, in the middle of, and 1 mm below the void, respectively. Note: As can be seen in the profiles on the top row, the attenuation coefficient of the weld is 10% smaller than that of the pipe. This difference is so small that it is difficult to see in the grayscale image, but it serves a realistic violation of our assumption of only two different materials and hence tests the robustness of the proposed reconstruction algorithm.

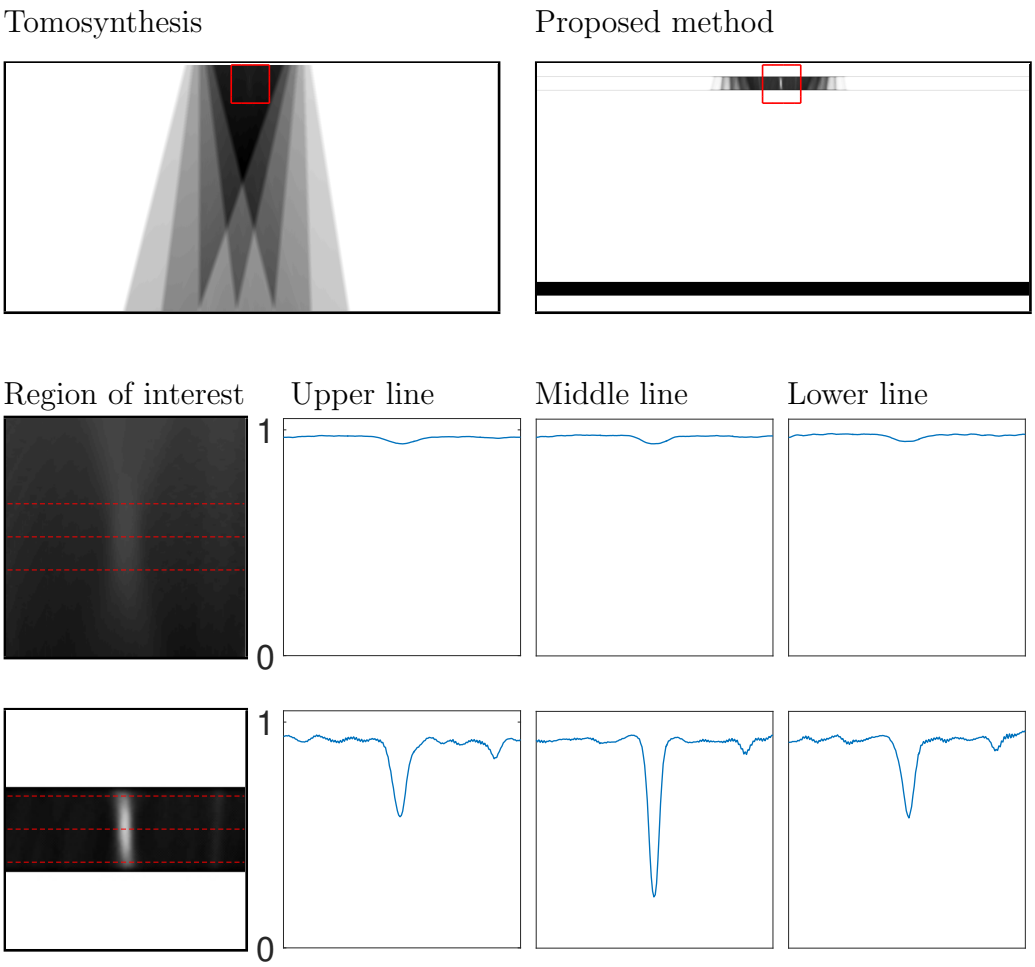

Figure 4: Real data results for an aluminium pipe with a void of 0.5 mm diameter. Top: Reconstructions by tomosynthesis and the proposed TVR-DART variant. Middle row: the region of interest enclosed be the red rectangle in the tomosynthesis reconstruction and the reconstruction profiles on lines indicated by the red dashed lines. Bottom: Same results as in the middle row but for the reconstruction computed by the proposed method.

4. Discussion and conclusion

The numerical results shown demonstrate that the proposed TVR-DART variant is able to significantly improve the accuracy of depth information when compared to standard tomosynthesis. This is highlighted by the reconstruction profiles shown above, below and in the middle of the void in Figures 3 and 4.

The difference between the proposed method and tomosynthesis is not as clear in the real-data case as in the simulated data test case. However, in the real data test case the void was really small with only 0.5 mm diameter. In many practical applications, such as weld evaluation, defects smaller than 1 mm in diameter are of no interest.

The results with the simulated data illustrate that the a priori information of the shape of the pipe and/or weld need not be perfect. As can be seen from Figures 2 and 3, minor inaccuracies in the shape of the weld seem not to significantly affect the image quality in the region of interest.

The choice of the parameters K, τ_g and α is critical to the reconstruction quality, so they should be chosen carefully for the application in question.

In addition to voids (pores), there are many other types of welding defects such as slag inclusions. They could also be found with the proposed method by including them as the third material in the model. Further studies using real X-ray data of welds with actual defects would be valuable.

Acknowledgements

This work was funded by Business Finland (decision number 528/31/2015), Academy of Finland (Finnish Centre of Excellence in Inverse Problems Research 2012–2017, decision number 250215; Finnish Centre of Excellence in Inverse Modelling and Imaging 2018–2025, decision number 312339), and three Finnish companies: Ajat Ldt, Innomentarium Ltd and KaVo Kerr Group Ltd. The authors also thank Kemppi Ltd for helpful discussions related to welding process.

[1] U. Ewert, B. Redmer, D. Walter, K. Thiessenhusen, C. Bellon, P. Nicholson, A. Clarke, K. Finke-Härkönen, J. Scharfschwerdt, K. Rohde, X-ray tomographic in-service-testing of circumferential pipe welds - the european project tomoweld, 19th World Conference on Non-Destructive Testing.

[2] M. E. Davison, The ill-conditioned nature of the limited-angle tomography problem, SIAM Journal on Applied Mathematics 43 (1983) 428–448.

[3] A. K. Louis, Incomplete data problems in X-ray computerized tomography I. singular value decomposition of the limited angle transform, Numerische Mathematik 48 (1986) 251–262.

[4] F. Natterer, The mathematics of computerized tomography, Vol. 32, John Wiley & Sons, Chichester, USA, and B. G. Teubner, Stuttgart, Germany, 1986.

[5] E. Quinto, Singularities of the X-ray transform and limited data tomography in $\mathbb{R}^2$ and $\mathbb{R}^3$, SIAM Journal on Mathematical Analysis 24 (1993) 1215–1215.

[6] J. Mueller, S. Siltanen, Linear and Nonlinear Inverse Problems with Practical Applications, Computational Science and Engineering, SIAM, 2012.

[7] A. H. Delaney, Y. Bresler, Globally convergent edge-preserving regularized reconstruction: an application to limited-angle tomography, IEEE Transactions on Image Processing 7 (2) (1998) 204–221.

[8] M. Persson, D. Bone, H. Elmqvist, Total variation norm for three-dimensional iterative reconstruction in limited view angle tomography, Physics in Medicine and Biology 46 (2001) 853–866.

[9] V. Kolehmainen, S. Siltanen, S. Järvenpää, J. Kaipio, P. Koistinen, M. Lassas, J. Pirttilä, E. Somersalo, Statistical inversion for medical X-ray tomography with few radiographs: II. application to dental radiology, Physics in Medicine and Biology 48 (2003) 1465–1490.

[10] S. Siltanen, V. Kolehmainen, S. Järvenpää, J. P. Kaipio, P. Koistinen, M. Lassas, J. Pirttilä, E. Somersalo, Statistical inversion for medical X-ray tomography with few radiographs: I. general theory, Physics in medicine and biology 48 (2003) 1437–1463.

[11] M. Rantala, S. Vänskä, S. Järvenpää, M. Kalke, M. Lassas, J. Moberg, S. Siltanen, Wavelet-based reconstruction for limited-angle X-ray tomography, Medical Imaging, IEEE Transactions on 25 (2) (2006) 210–217.

[12] E. Y. Sidky, C.-M. Kao, P. Xiaochuan, Accurate image reconstruction from few-views and limited-angle data in divergent-beam CT, Journal of X-Ray Science and Technology 14 (2) (2006) 119–139.

[13] V. Kolehmainen, M. Lassas, S. Siltanen, Limited data X-ray tomography using nonlinear evolution equations, SIAM Journal on Scientific Computing 30 (3) (2008) 1413–1429.

[14] J. Frikel, A new framework for sparse regularization in limited angle X-ray tomography, in: Biomedical Imaging: From Nano to Macro, 2010 IEEE International Symposium on, 2010, pp. 824 –827. doi:10.1109/ISBI.2010.5490113.

[15] S. Yoon, A. R. Pineda, R. Fahrig, Simultaneous segmentation and reconstruction: A level set method approach for limited view computed tomography, Medical Physics 37 (5) (2010) 2329–2340. doi:10.1118/1.3397463.
URL http://link.aip.org/link/?MPH/37/2329/1

[16] M. I. Haith, P. Huthwaite, M. J. Lowe, Defect characterisation from limited view pipeline radiography, NDT & E International 86 (2017) 186 – 198. doi:https://doi.org/10.1016/j.ndteint.2016.12.007.
URL http://www.sciencedirect.com/science/article/pii/S0963869516302808

[17] G. Jones, P. Huthwaite, Limited view x-ray tomography for dimensional measurements, NDT & E International 93 (2018) 98 – 109. doi:https://doi.org/10.1016/j.ndteint.2017.09.002.
URL http://www.sciencedirect.com/science/article/pii/S0963869517302074

[18] M. Goswami, S. Shakya, A. Saxena, P. Munshi, Reliable reconstruction strategy with higher grid resolution for limited data tomography, NDT & E International 72 (2015) 17 – 24. doi:https://doi.org/10.1016/j.ndteint.2014.09.012.
URL http://www.sciencedirect.com/science/article/pii/S0963869515000043

[19] C. Schorr, L. Drr, M. Maisl, T. Schuster, Registration of a priori information for computed laminography, NDT & E International 86 (2017) 106 – 112. doi:https://doi.org/10.1016/j.ndteint.2016.12.005.
URL http://www.sciencedirect.com/science/article/pii/S0963869516302687

[20] N. A. B. Riis, J. Frøsig, Y. Dong, P. C. Hansen, Limited-data x-ray ct for underwater pipeline inspection, Inverse Problems.

[21] X. Zhuge, W. J. Palenstijn, K. J. Batenburg, TVR-DART: A more robust algorithm for discrete tomography from limited projection data with automated gray value estimation, IEEE Transactions on Image Processing 25 (1) (2016) 455–468. doi:10.1109/TIP.2015.2504869.

[22] Y. Liu, A. Beyer, P. Schuetz, J. Hofmann, A. Flisch, U. Sennhauser, Cooperative data fusion of transmission and surface scan for improving limited-angle computed tomography reconstruction, NDT & E International 83.

[23] J. Barzilai, J. Borwein, Two-point step size gradient methods, IMA Journal of Numerical Analysis 8 (1) (1988) 141–148.

[24] W. van Aarle, W. J. Palenstijn, J. Cant, E. Janssens, F. Bleichrodt, A. Dabravolski, J. D. Beenhouwer, K. J. Batenburg, J. Sijbers, Fast and flexible x-ray tomography using the astra toolbox, Opt. Express 24 (22) (2016) 25129–25147. doi:10.1364/OE.24.025129.
URL http://www.opticsexpress.org/abstract.cfm?URI=oe-24-22-25129

[25] W. van Aarle, W. J. Palenstijn, J. D. Beenhouwer, T. Altantzis, S. Bals, K. J. Batenburg, J. Sijbers, The astra toolbox: A platform for advanced algorithm development in electron tomography, Ultramicroscopy 157 (2015) 35 – 47. doi:https://doi.org/10.1016/j.ultramic.2015.05.002.
URL http://www.sciencedirect.com/science/article/pii/S0304399115001060